

Date of publication xxxx 00, 0000, date of current version xxxx 00, 0000.

Digital Object Identifier 10.1109/ACCESS.2017.DOI

A Highly-Efficient Fuzzy-based Controller with High Reduction Inputs and Membership Functions for a Grid-connected Photovoltaic System

LOTFI FARAH¹, AMIR HUSSAIN², (Senior Member, IEEE), ABDELFAHEH KERROUCHE², COSIMO IERACITANO³, JAMIL AHMAD⁴, (Senior Member, IEEE), and MUFTI MAHMUD⁵, (Senior Member, IEEE)

¹University Badji Mokhtar Annaba Algeria, Genie Électromécanique Laboratory, Electromécanique Department (email: lotfi.farah@univ-annaba.dz)

²School of Computing, Edinburgh Napier University, Edinburgh EH10 5DT, Scotland, United Kingdom (email: a.hussain@napier.ac.uk, A.Kerrouche@napier.ac.uk)

³DICEAM, University Mediterranea of Reggio Calabria, Via Graziella Feo di Vito, 89124, Italy (email: cosimo.ieracitano@unirc.it)

⁴Kohat University of Science and Technology (KUST), Khyber Pakhtunkhwa (KPK), Pakistan (email: jamil.ahmad@kust.edu.pk)

⁵Department of Computing & Technology, Nottingham Trent University, Clifton, Nottingham NG11 8NS, United Kingdom (e-mail: muftimahmud@gmail.com, mufti.mahmud@ntu.ac.uk)

Corresponding author: L. Farah (email: lotfi.farah@univ-annaba.dz).

ABSTRACT Most conventional Fuzzy Logic Controller (*FLC*) rules are based on the knowledge and experience of expert operators: given a specific input, *FLCs* produce the same output. However, *FLCs* do not perform very well when dealing with complex problems that comprise several input variables. Hence, an optimization tool is highly desirable to reduce the number of inputs and consequently maximize the controller performance, leading to easier maintenance and implementation. This paper, presents an enhanced fuzzy logic controller applied to a photovoltaic system. Specifically, both inputs and membership functions are reduced, resulting in a Highly Reduced Fuzzy Logic Controller (*HRFLC*), to model a 100kW grid-connected Photovoltaic Panel (*PV*) as part of a Maximum Power Point Tracking (*MPPT*) scheme. A *DC* to *DC* boost converter is included to transfer the total energy to the grid over a three-level Voltage Source Converter (*VSC*), which is controlled by varying its duty cycle. *FLC* generates control parameters to simulate different weather conditions. In this study, only one input representing the current variation (ΔI) of the *FLC* is used to provide an effective and accurate solution. This reduction in simulation inputs results in a novel *HRFLC* which simplifies the solar electric system design with output Membership Functions (*MFs*). Both are achieved by grouping two rules instead of using an existing state-of-the-art method with twenty-five *MFs*. To the best of our knowledge, this is the first *FLC* able to provide such rules compression. Finally, a comparison with different techniques such as Perturb and Observe (*P&O*) shows that *HRFLC* can improve the dynamic and the steady state performance of the *PV* system. Notably, experimental results report a steady state error of 0.119%, a transient time of 0.28s and an *MPPT* tracking accuracy of 0.009s.

INDEX TERMS Boost Converter, Current Variation, Grid Connection, High Reduced Fuzzy Based *MPPT* Controller (*HRFLC*), Photovoltaic Panel, Three level *VSC*.

Nomenclature

Variables

$\Delta E(t)$	Error Variation
ΔI	Current Variation
ΔP	Power Variation
ΔV	Voltage Variation
C	Capacitor Value

D	Duty Cycle
dP_{PV}/dI_{PV}	Power derivation by current
$E(t)$	Error
G	Irradiation
I_{in}	Input Current
I_{out}	Output Current
I_{Ph}	Photo Current

I_{PV}	Light Generated Current
L	Induction Value
Le	VSC Level
N	IGBTs Number
R_o	Output Resistance
R_{eq}	Equivalent Resistance
R_{in}	Input Resistance
T	Temperature
V_o	DC/DC Output Voltage
V_{ab}	Output Line to Line Voltage of the VSC
$V_{carrier}$	Carrier Voltage
V_{in}	DC/DC Input Voltage
V_{PV}	Module Output Voltage
X_i	Input Fuzzy Data
Y_{COG}	Output Fuzzy Controller Value
Y_i	Membership Function Value
Acronyms	
ADC	Analogic to Digital Converter
AI	Artificial Intelligence
$ANFIS$	Adaptive Neuro Fuzzy Inference System
ANN	Artificial Neural Network
COG	Center Of Gravity
$DC - DC$	Direct Current to Direct Current
FIS	Fuzzy Inference System
FLC	Fuzzy Logic Controller
HC	Hill Climbing
Hi	High
$HRFLC$	Highly Reduced Fuzzy Logic Controller
IE	Initial Error
$InCon$	Incremental Conductance
Lo	Low
MF	Membership Function
MPP	Maximum Power Point
$MPPT$	Maximum Power Point Tracking
NPC	Neutral Point Clamped
$P\&O$	Perturb & Observe
P_{MPP}	Power value at the Maximum Power Point
P_{PV}	Panel Power
PB	Positive Big
PID	Proportional, Integral and Derivation
PS	Positive Small
PV	Photo Voltaic
PVG	Photo Voltaic Generator
PWM	Power Wave Modulation
$S\&H$	Sample and Hold
SSE	Steady State Error
ST	Steady Time
$TOANC$	Third Order Adaptative Neuro Fuzzy Controller
TrC	Triangular Carrier
TT	Tracking Time
VSC	Voltage Source Converter
Constants	
A	PV cell ideal factor
f	Frequency
I_{CSr}	Short Circuit Current
I_{mp}	Optimal Current

I_o	Saturation Current
k	Boltzmann Constant
N_P	Parallel connected cells Number in a PV Module
N_s	Series connected cells Number in a PV module
P_m	Maximal Module Power
q	The electron charge
R_s	Serial Resistance in PV Cell
R_{sh}	Parallel Resistance in PV Cell
V	Voltage Value
V_{dc}	Input VSC Voltage
V_{mp}	Optimal Voltage Module
V_{oc}	PV Module Open Circuit Voltage
V_{ref}	Reference Voltage

I. INTRODUCTION

IN the last few years, there is a great deal of interest worldwide in searching new energy sources able to replace the dwindling fossil fuels. In this context, solar energy turned out to be the most attractive alternative due to its advantages of being cleaner, renewable and inexhaustible [1]– [2]. The main function of Photovoltaic (*PV*) is to transform the solar irradiance into electric power. However, the generated power from *PV* depends not only on irradiance but also on other factors such as temperature and spectral properties of sunlight [3]– [5]. These conditions need to be controlled in order to allow a *PV* panel to operate at the Maximum Power Point (*MPP*). It is well known from *MPP* theory that the power delivered to the load is maximum only when the internal impedance is equal to the load impedance. For this reason, a *DC-DC* converter is used. In the literature, many techniques have achieved this adaptation between the *PV* panel and the load impedance at different atmospheric conditions such as the well-known Perturb and Observe (*P&O*) [3]– [6], including the Incremental Conductance technique (*InCon*). *P&O* is cost effective and relatively easy to implement for controlling directions. However, this technique shows trade-offs between tracking speed and steady state accuracy to control atmospheric perturbations [3]– [7]. To overcome this problem, several solutions have been proposed [8]– [10]. In particular, it is worth mentioning that the perturbation step increases when the working point is far from the *MPP*, since the steps are proportional to the ratio dP_{PV}/dV_{PV} (and vice-versa) [8]– [11].

In the recent years, with the emergence and development of Artificial Intelligence (*AI*) [12], many applications such as, text mining to biology, financial forecasting, rehabilitation systems, trust management and medical diagnosis [13]– [21] have been efficiently improved. Furthermore, *AI* also provided effective and robust solutions to the field of electro-control systems by developing *PID*, fuzzy logic [11], [22]– [38] and Artificial Neural Networks (*ANNs*) [39]– [41] based-control approaches. A comprehensive fuzzy system has been used by [11] to intelligently and adaptively tune the *PID* gain. Adaptive neuro-fuzzy controller system has been proposed for controlling *MPPT* with constant temperature and varying irradiance [22]– [25]. Recently, fuzzy logic is

used in several applications due to its simplicity and its interpretability. Note that the main advantage of such technique is the addition or withdrawal of membership functions (*MFs*) without rehabilitation or re-learning. Fuzzy logic allows to model natural language rules and also complex dynamic systems. For this reason, fuzzy-based *MPPT* algorithms have gained a great deal of attention [11], [22]– [31]. Notably, high tracking performance have been obtained by using fuzzy-based *MPPT* [11], [22]– [31]. Hitherto, most of the works used two inputs and one output with five *MFs* to generate twenty-five rules [22]– [32]. Others used one output and two inputs of seven *MFs*, resulting in forty-nine rules [22]. In [23], two inputs were used with three *MFs*, yielding nine rules. Vicente Salas et al. [42] employed the variation of current as the unique input in *MPPT* controller. Specifically, the authors used one input with two *MFs*, one output with two *MFs* and only two rules. To the best of our knowledge, this was the first approach able to provide a significant reduction in number of inputs and *MFs*. It is to be noted, as reported in the literature, that different inputs can be selected. In particular, some used the temperature and irradiance variation [23], whereas others used error variation and momentum [24]– [28]. In [32], the proposed fuzzy controller employed different input variables, such as: (1) slope of solar power vs. solar voltage and slope changes; (2) slope and power variation (ΔP); (3) ΔP and voltage variation (ΔV); (4) ΔP and current variation (ΔI); (5) sum of conductance and conductance increment; (6) sum of conductance arctangent angles and increment conductance arctangent. In [41] the inputs were dP_{PV}/dI_{PV} and the error $E(t)$ (defined as $P_{MPP} - P_{PV}$); or, $E(t)$ and error variation ($\Delta E(t)$). However, for computational reasons, the best inputs turn out to be the ΔP_{PV} and ΔV_{PV} (or ΔI_{PV}), power variation and voltage (or current) variation, respectively [22]– [41]. Hence, as reported in the aforementioned works, all controllers based on *MPPT* used at least two inputs. In contrast, this paper propose a highly-efficiency fuzzy-based *MPPT* controller with high reduction inputs and *MFs* for a grid-connected photovoltaic system. Notably, only two *MFs* were used. Furthermore, $\Delta I_{PV} = (I_{PV}(k) - I_{PV}(k-1))$ is selected as unique input. Consequently, the calculation time, the number of variables and the circuitry (Analog to Digital Converter (*ADC*), Sample and Hold (*S&H*), filter, etc..) are significantly reduced. Moreover, the proposed fuzzy-based controller approach is able to decrease the tracking time and concurrently increase the tracking accuracy as compared with other state-of-the-art controllers.

The rest of the paper is organized as follows: in Section II mathematical details of a *PV* panel are introduced; in Section III the design of the *DC-DC* converter is presented; Section IV and V describe the fuzzy based *MPPT* controller and the Pulse Width Modulation (*PWM*) used for the three level voltage source converter, respectively. In Section VI the model and simulation of the *PV* system with *HRFLC* based *MPPT* controller is presented. In Section VII the experimental results are discussed and in Section VIII conclusions are

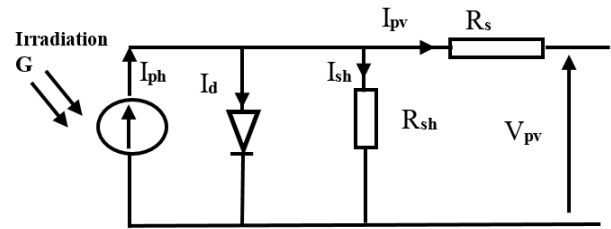


FIGURE 1. Circuit model of a photovoltaic cell [35].

addressed.

II. MATHEMATICAL MODELING FOR A PHOTOVOLTAIC PANEL

A solar cell is composed of two types of semiconductors, called *p*-type and *n*-type. Photovoltaic transformation occurs when solar cell is exposed to sunlight, by converting the electromagnetic solar irradiance to electricity. Incident irradiance produces proportional electron-hole pairs if their energy is greater than the energy of the semiconductor’s band-gap. Fig. 1 shows the circuit model of a standard photovoltaic model. The photocurrent I_{Ph} is the current source of the *PV* cell, generated when irradiation G occurs [42] [48]. Intrinsic shunt and series *PV* cell resistances are R_{sh} and R_s , respectively. It is to be noted that R_{sh} assumes typically high values and vice-versa, R_s low values. *PV* cells associated to larger units result in *PV* modules; these, interconnected together in parallel-series configurations, lead to the production of *PV* arrays. Equation (1) shows the current output when the mathematical model of the *PV* panel is simulated [43].

$$I_{PV} = N_P I_{Ph} - N_P * I_0 \left[\exp\left(\frac{q * (V_{PV} + I_{PV} R_s)}{N_s A k T}\right) - 1 \right]. \quad (1)$$

In this work, the SunPower SPR-305-WHT *PV* panel is used with the following characteristics: Maximal Module Power (P_m) of 305W, optimal voltage (V_{mp}) of 54.7V, optimal current (I_{mp}) of 5.58A, saturation current (I_0) of $1.1753e^{-08}$ A, photo-current (I_{Ph}) of 5.9602A, short circuit current (I_{Csr}) of 5.96A, open circuit voltage (V_{oc}) of 64.2V, serial resistance (R_s) of 0.037998Ω , parallel resistance (R_{sh}) of 993.51Ω and number of cells equal to 96. As regards the *PV* array, its characteristics are: serial modules number of 5 and parallel modules number of 66. Hence, the *PV* has a power of about 100kW, obtained as follows $66 \times 5 \times 305W = 100650W = 100.65kW$. Irradiance of $1kW/m^2$ and cell temperature of $25^\circ C$ are the electrical specifications under test conditions. I-V and P-V curves of the array are depicted in Fig. 2. Here, the *PV* panel is directly connected to a *DC-DC* converter. This converter is an impedance adapter and allows to transfer the power captured from the *PV* panel to the grid toward a three-level voltage source converter.

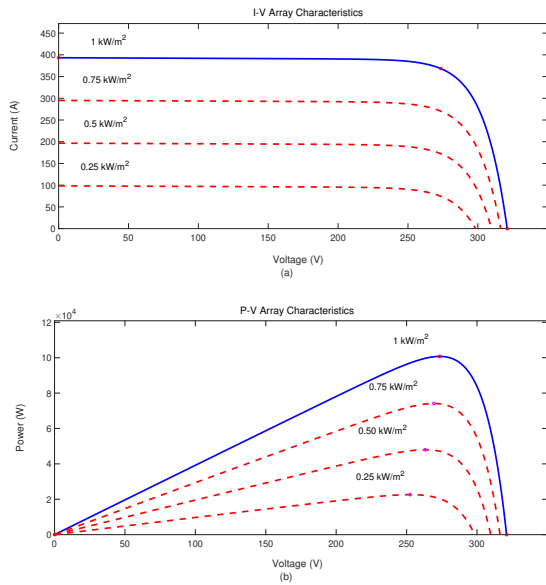


FIGURE 2. Array characteristics curves I-V (a) and P-V (b).

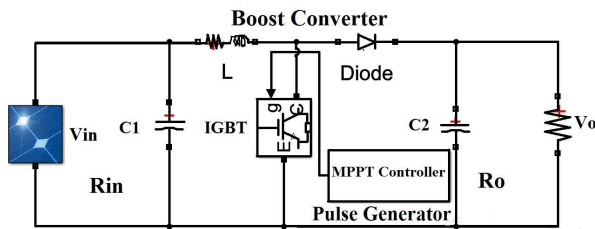


FIGURE 3. The DC-DC Boost converter.

III. DESIGN THE DC-DC CONVERTER

A simple *DC-DC boost* converter transfers the power consumption from the *PV Generator (PVG)* to the load, when the adaptation condition (between *PVG* and load) occurs. The adaptation is characterized by an adequate duty cycle signal ($0 < D < 1$). Note that the *PWM* signal controls the valve gate, *IGBT*, in the boost converter. The wiring Simulink diagram of the *DC-DC boost* is shown in Fig. 3.

The relationship between inputs and outputs variables of the boost converter is represented by the following equations [44]:

$$V_o = V_{in}/(1 - D). \quad (2)$$

$$I_{out} = (1 - D)I_{in}. \quad (3)$$

whereas, Equation (4) shows the equivalent resistance (R_{eq}) of the *DC-DC boost* converter:

$$R_{eq} = R_{in}(1 - D)^2. \quad (4)$$

The maximum power is transferred to the load when R_{eq} is equal to the output resistance (R_o) of the *PV* system

[45]– [46]. Hence, according to the maximum power transfer theorem the duty cycle can be obtained as follows:

$$R_{in} = V_{in}/I_{in} = R_o(1 - D)^2 \implies D = 1 - \sqrt{\frac{R_{in}}{R_o}}. \quad (5)$$

Inductor (L) and capacitor (C) functions of the *DC-DC boost* converter are instead defined as:

$$L = \frac{(V_o - V_{in})V_{in}}{f(\Delta I)V_o}. \quad (6)$$

$$C = \frac{(V_o - V_{in})I_{out}}{f(\Delta V)V_o}. \quad (7)$$

where D is the duty cycle; f is the frequency (5 kHz in this study); V_{in} and V_o are the inputs and outputs voltages, respectively; ΔI and ΔV are the current and voltage ripple. Here, $L = 5e^{-3}\text{H}$ and $C = 12000e^{-06}\text{F}$. Fig. 4 depicts the I-V curve of the panel studied with different working zone. In particular, A-B area denotes the buck working zone, B-C the boost working zone and finally A-C the buck-boost working zone [47]. In this work, the boost converter’s working zone (B-C) is the most important and, ΔI is the variable of greatest interest. Note that in Fig. 4, B is the *MPP* point and C is the open circuit point. At the B point $R_o = R_{in}$. Furthermore, in this area, $R_o \gg R_{in}$ with $R_{in} = R_o(1 - D)^2$. In order to have a stable voltage at the grid, the *VSC* voltage must be stable and constant. In this study, the voltage supplied to the *VSC* is kept constant ($V = 500\text{V}$) as shown in Fig. 10.

IV. FUZZY BASED MPPT CONTROLLER

A. FUZZY INFERENCE SYSTEM

A standard Fuzzy Inference System (*FIS*) consists of three modules, as shown in Fig. 6. In the first stage, called *fuzzification*, input variables are expressed in linguistic variables by assigning a *MF*. Secondly, *IF-THEN* rules are applied. Finally, in the *defuzzification* step, linguistic variables are transformed into specific output values and parameters are adjusted based on the input-output data relation [22]– [33].

B. FUZZY LOGIC CONTROLLER

A Fuzzy Logic Controller (*FLC*) is based on a *FIS* [32]. In fuzzification, the selected linguistic variables are the Positive Small (*PS*) and the Positive Big (*PB*). These linguistic values attribute a fuzzy score to the input. In this paper, both input and output *MFs* are triangular for its simplicity and ease of implementation (Fig. 5). It is to be noted that a high number of *MFs* lead to an increase of rules and consequently, the control program is difficult to implement.

In this work, two rules are necessary to efficiently develop the control and provide accurate results. Moreover, only one input is used for the *FLC*, that is the current variation ΔI_{PV} , defined as follows:

$$\Delta I_{PV}(n) = I_{PV}(n) - I_{PV}(n - 1). \quad (8)$$

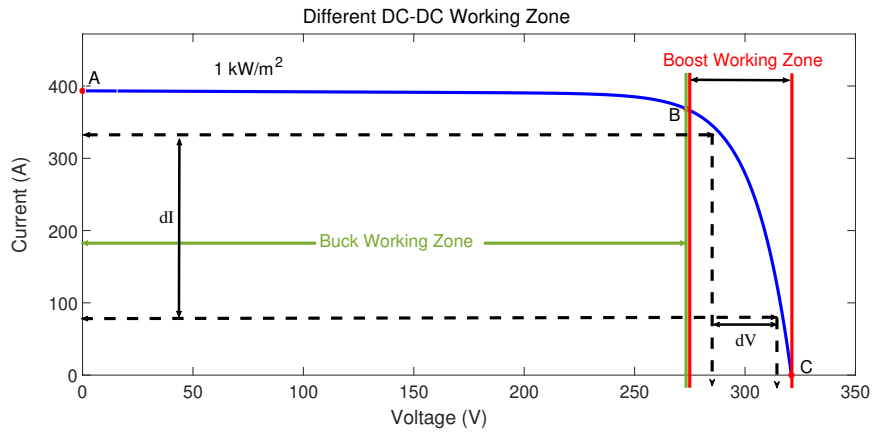


FIGURE 4. I-V curve of the working zone of the buck-boost converter.

TABLE 1. Fuzzy rules.

ΔI_{PV}	D
PS	Hi
PB	Lo

Table 1 reports the rules used in this paper. As can be seen only two *MFs* are involved. In contrast, in [22]– [32] higher number of rules are employed (i.e., from 9 to 49). Note that the rules define the relationship between ΔI and D , represented by the IF-THEN instructions. For example, if the change in current is *PS* then D will be high.

$$Y_{COG} = \frac{\sum_{i=1}^n Y_i(X_i)X_i}{\sum_{i=1}^n Y_i(X_i)}. \quad (9)$$

where *COG* stands for Centre Of Gravity. The final level of *FLC* is the defuzzification able to produce a signal that controls the *MPP*. The *PV* panel current and the *PV* current variation ΔI are illustrated in Fig. 7. As can be seen, ΔI is always positive in all irradiance variations.

V. THREE LEVEL PWM VOLTAGE SOURCE CONVERTER

In the literature, several multilevel inverter topologies have been introduced, such as the diode clamped multilevel inverter, the flying capacitor multilevel inverters, and the cascaded H-bridge multilevel inverter. The most used is the well-known Neutral Point Clamped (*NPC*) [49]– [50]. In this paper, a three-level Voltage Source Converter (*VSC*) is employed, since it is suitable for higher voltage inverters and provides the following advantages than a common two-level inverters: i) low output current ripples; ii) reduced harmonic power as a result of a smaller output voltage that leads to cleaner AC output waveform; iii) the IGBTs are subjected to the half of the bus voltage; iv) the *NPC* inverter is characterized by a low common-mode and line-to-line voltage step. However, the three-level *VSC* provides a double effective switching frequency, an augmented number of IG-

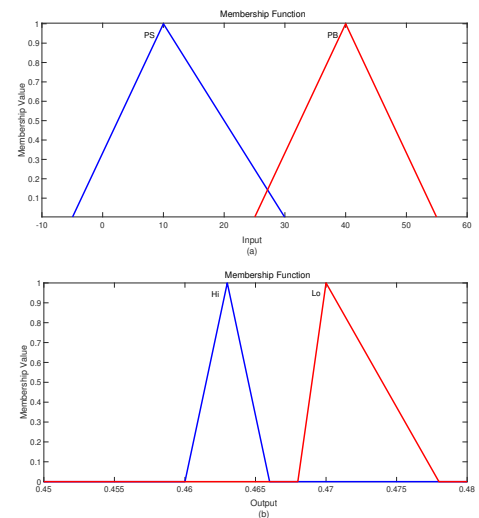


FIGURE 5. Input (a) and output (b) Fuzzy Membership Functions (MFs).

BTs and a complex control strategy while increasing in level. This means that the cost and magnitude of its components is higher than the well-known two-level inverters, due to the reduced output voltage steps. In order to achieve such voltages, N IGBTs are added in each level:

$$N = 2(Le - 1). \quad (10)$$

where Le the desired level. In this study $Le = 3$, so, four IGBTs are needed for one leg, as shown in Fig. 8. In this topology, half of the voltage ($V_{dc}/2$) is applied to the IGBT achieved by the two equal capacitors in series. Furthermore, two clamp diodes in each leg are responsible for driving the half voltage to each specific IGBT [49]. For each of the three phases, produced in each leg (Fig. 8), the output voltage switches between $-\frac{V_{dc}}{2}$ and $\frac{V_{dc}}{2}$. These voltages are obtained by turning on at the same time: 1) A1 and A2; 2) A2 and A3; 3) A3 and A4 as reported in

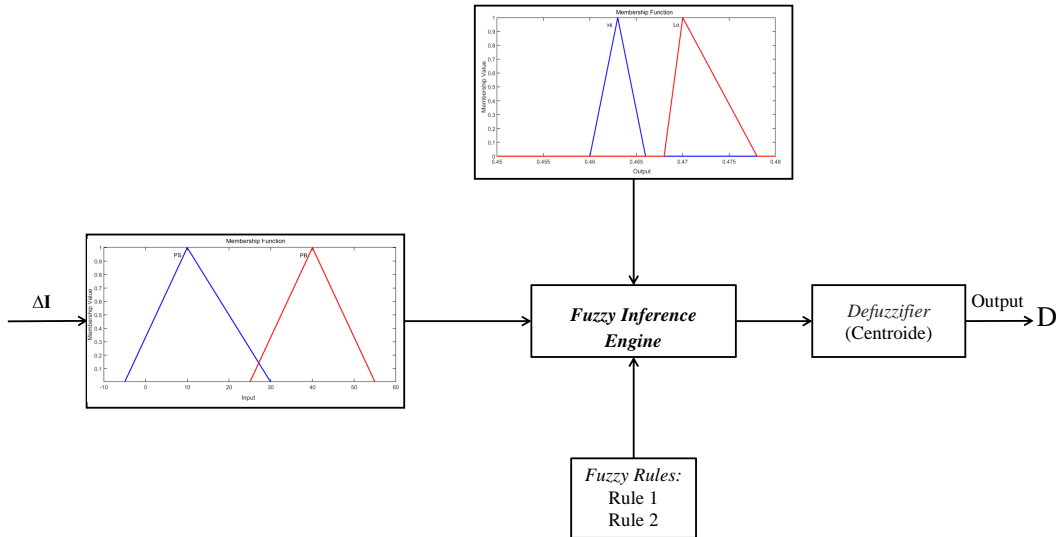


FIGURE 6. Proposed HRFLC based MPPT controller diagram.

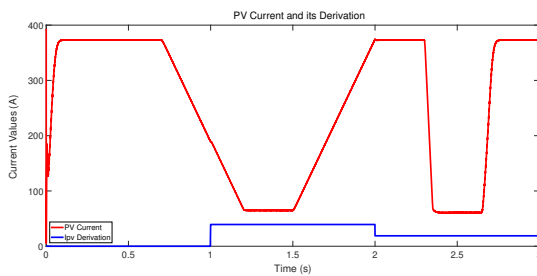


FIGURE 7. PV panel current and its derivation.

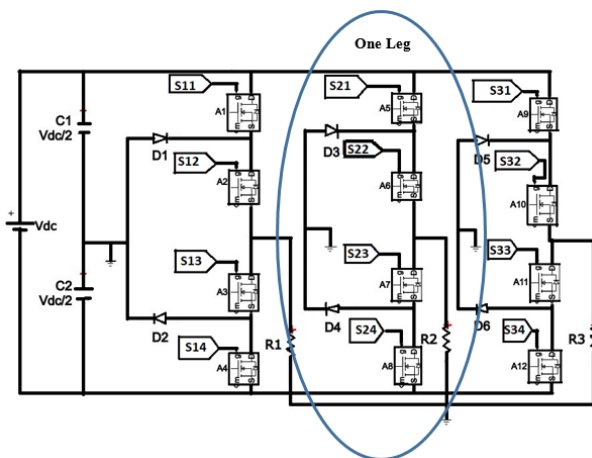


FIGURE 8. Three phase voltage source converter.

Table 2, where A1, A2, A3 and A4 are the IGBTs in each leg. Such switching control options generate $\frac{V_{dc}}{2}$, zero and $-\frac{V_{dc}}{2}$. After filtering, a sine waveform is obtained at the AC output. The connection to the 0 Volt (neutral point) is assured by the clamp diodes D3 and D4. It can be seen from Table 2 that A2 and A3 conduct more than A1 and A4 causing a conduction loss on A2 and A3 and a switching loss on A1 and A4 [50]. The capacitors C1 and C2 are coupled in series to generate the neutral point (0 Volt). Setting an equal voltage in the capacitors and establishing a neutral tension in the mid-point is important for the proper operation of NPC. Any unbalance voltage in the capacitors will affect directly the AC output. In this work, the sine triangular PWM waveform method is used [50]– [51]. Specifically, in order to create the sine-carrier PWM, a comparison of the three references control signals, the pure sine waveform with 120° , and the two triangular carrier waves $TrC1$ and $TrC2$ is performed. Fig. 9 shows the comparison of one reference with the two triangular carriers. Specifically, the comparison of the sine waveform with $TrC1$ and $TrC2$ produces the on/off switch of A1 and A2, respectively. The switching on and off of A3 and A4 are the inverse of A1 and A2, respectively.

TABLE 2. IGBTs switching options.

IGBT				V_{out}
A1	A2	A3	A4	
1	1	0	0	$V_{dc}/2$
0	1	1	0	0
0	0	1	1	$-V_{dc}/2$

The corresponding control signals for the IGBTs can be

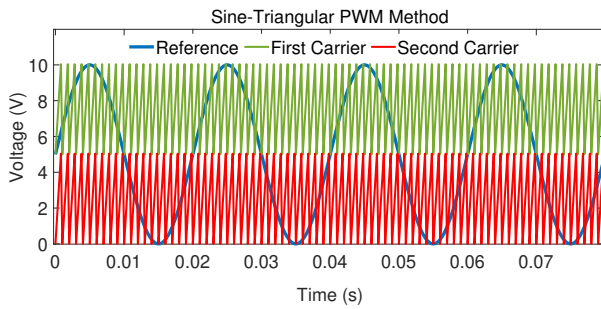


FIGURE 9. Comparison of the reference to two triangular carriers.

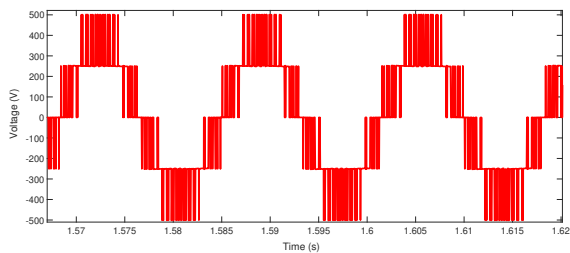


FIGURE 10. A zoom in VSC voltage V_{ab} .

expressed as follows:

$$V = \begin{cases} 1 & \text{if } V_{carrier} > V_{ref} \\ 0 & \text{if } V_{carrier} < V_{ref} \end{cases} \quad (11)$$

A zoom of the line-to-line voltage (V_{ab}), obtained at the VSC, is illustrated in Fig. 10. Here, the total harmonic distortion calculated for V_{ab} is 0.39%.

VI. MODELING AND SIMULATION OF PV SYSTEM WITH HRFLC BASED MPPT CONTROLLER

The simulation model of the incremental conductance technique was performed by using constant temperature and by varying irradiance. Fig. 11 depicts irradiance and temperature selected as input to the PV panel. Fig. 12 represents the proposed HRFLC of a PV panel connected to the grid. In particular, Fig. 12 (a) depicts the synoptic scheme of the panel connected to the grid toward the VSC with the High Reduced Fuzzy based MPPT controller; whereas, Fig. 12 (b) illustrates the global scheme of the PV panel connected to the grid toward the boost DC-DC converter and the VSC.

The power transfer between the PV panel and the boost DC-DC converter at 25°C is shown in Fig. 13 (a); while, comparison results with 40°C, 20°C are reported in Fig. 13 (b). The steady state error (SSE) and tracking time (TT) are shown in Fig. 14 and 15, respectively. Fig. 16 (a) depicts the Steady Time (ST), SSE and TT at 40°C; whereas, Fig. 16 (b) highlights ST, SSE and TT at 20°C.

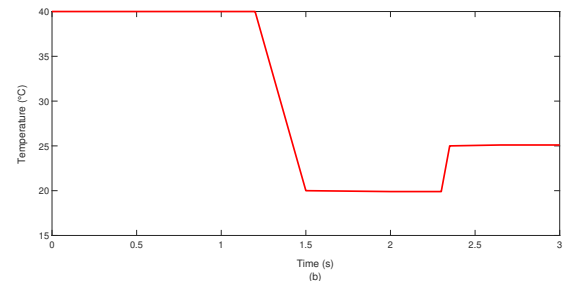
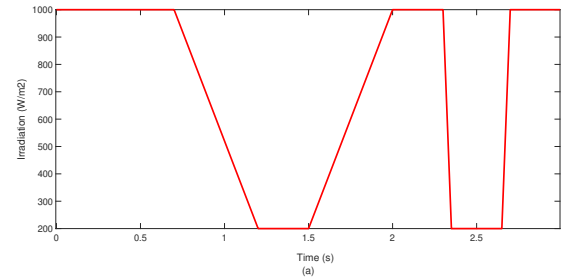


FIGURE 11. Irradiation (a) and temperature (b) as a function of time.

However, it is to be noted that a significant improvement was observed when the proposed HRFLC is employed. In particular, as regards the simulation carried out at 25°C, TT, ST and SSE were of 0.008s, 0.08s, 0.12 kW, respectively. This resulted in an error percentage of $0.12\text{kW}/100.65\text{kW} = 0.119\%$. In relation to the simulation at 20°C, instead, TT, ST and SSE were of 0.01s, 0.04s, 0.005kW, respectively. In this case the error percentage was $0.005\text{kW}/100.65\text{kW} = 0.0049\%$. Finally, as regards the experiment at 40°C, TT, ST and SSE were of 0.01s, 0.22s, 0.01kW, respectively, achieving an error of $0.01\text{kW}/100.65\text{kW} = 0.0099\%$ and an initial loss of about 9.5kW. The relationship between the boost power and grid power is depicted in Fig. 17. Specifically, Fig. 17(a) reports the simulation results at 25°C. In this scenario, TT is less than 0.004s (Fig. 19), ST is about 0.3s and SSE is of $100.54\text{kW} - 98.83\text{kW} = 1.71\text{kW}$ (Fig. 18), providing an error percentage of $1.71\text{kW}/100.65\text{kW} = 1.69\%$. Results show high tracking efficiency and a good performance due to the use of the three level converter. Note that this performance can be improved when using five level converter or more. As regards simulation performed at 20°C as shown in Fig. 20(b), the ST is 0.02s, TT is 0.005s, SSE is 2kW, resulting in an error of $2\text{kW}/100.65\text{kW} = 1.98\%$. As regards the 40°C simulation (see Fig. 20(a)), the following errors 0.03s TT, 0.17s ST and 1.4kW SSE were achieved, resulting an error percentage of $1.4\text{kW}/100.65\text{kW} = 1.39\%$. It is to be noted that in 20°C simulation there is a gain in power due to the materials characteristics of the PV. In this work, a stable voltage (i.e., 500V) was used to supply the VSC. By this assumption, the power variation depends on the current. Hence, the power estimated at the grid is 98.83kW and the power of the boost is 100.54kW, as shown in Fig. 18. The global power transfer between the PV panel and the grid at

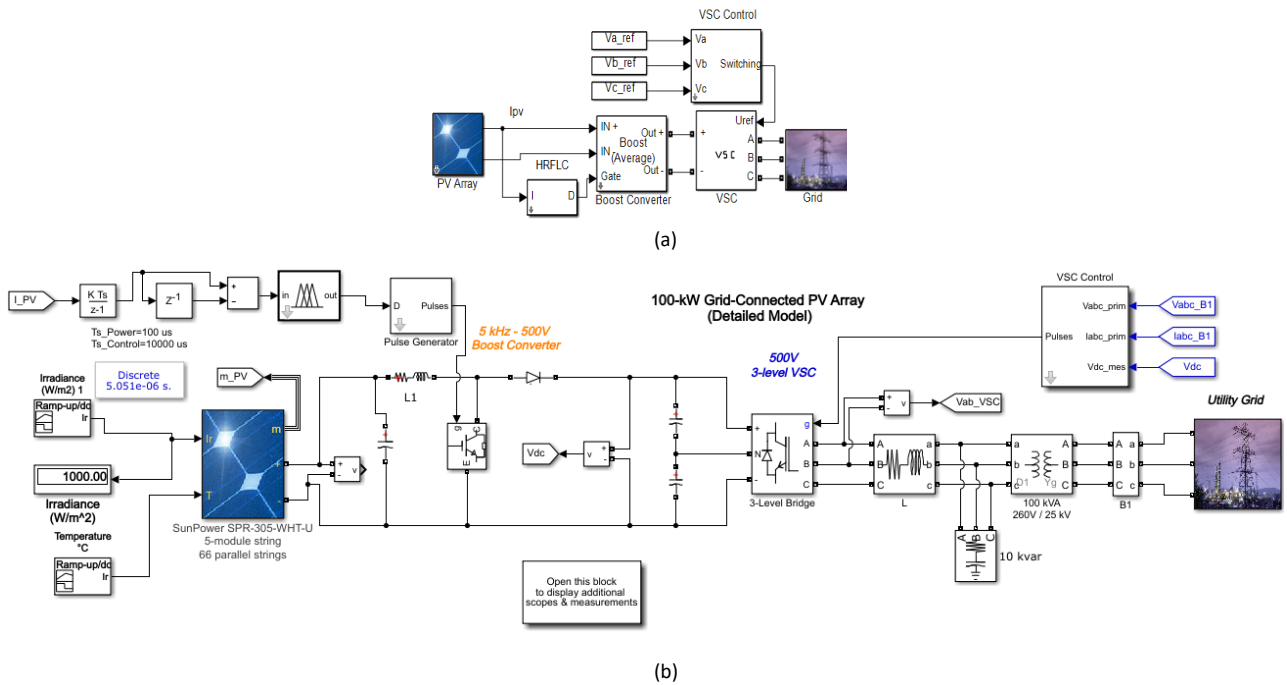


FIGURE 12. (a) Synoptic scheme of the PV panel connected to grid. (b) PV panel connected to grid with the HRFLC.

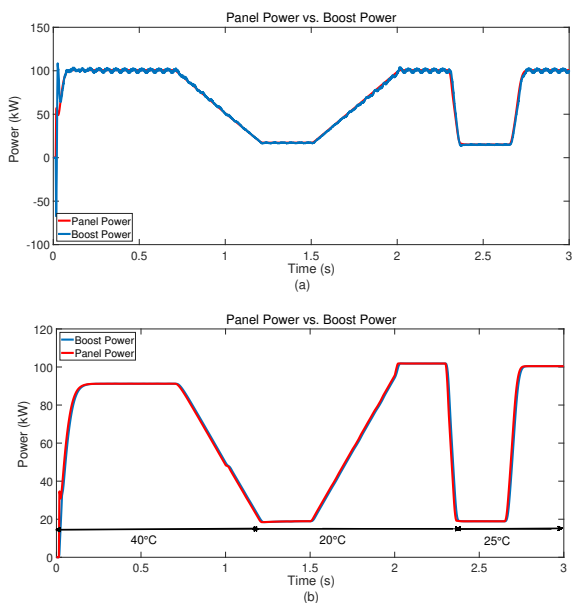


FIGURE 13. Simulation results of panel power and boost power at 25°C (a) and 40°C, 20°C, 25°C (b).

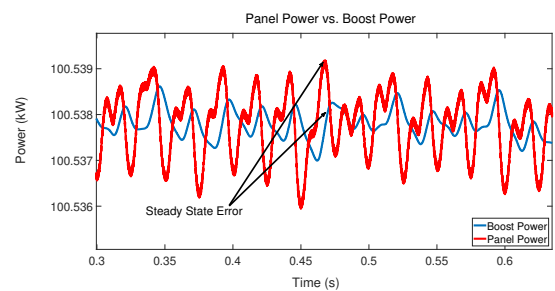


FIGURE 14. Simulation results of the steady state error between the panel power and boost power at 25°C.

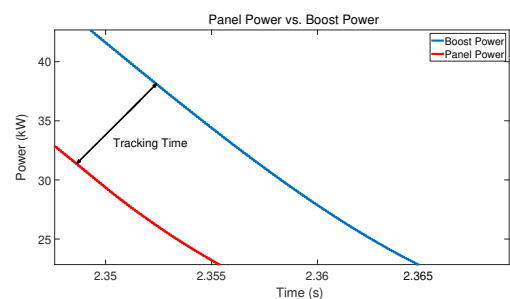


FIGURE 15. Simulation results of the tracking time between panel power and boost power at 25°C.

25°C is shown in Fig. 21. In this case, TT (Fig. 23), ST and SSE (Fig. 22) were of 0.005s, 0.09s and 1.82kW, respectively. For 20°C simulation, as shown in Fig. 24 (b) the ST was 0.02s, TT 0.02s, SSE 1.8kW, leading to an error percentage of 1.8kW/100.65kW=1.78%. Finally, as regards the 40°C simulation (Fig. 24 (a)) reports 0.04s of TT , 0.17s ST and 1.4kW

of SSE , resulting in an error of 1.4kW/100.65kW=1.39%.

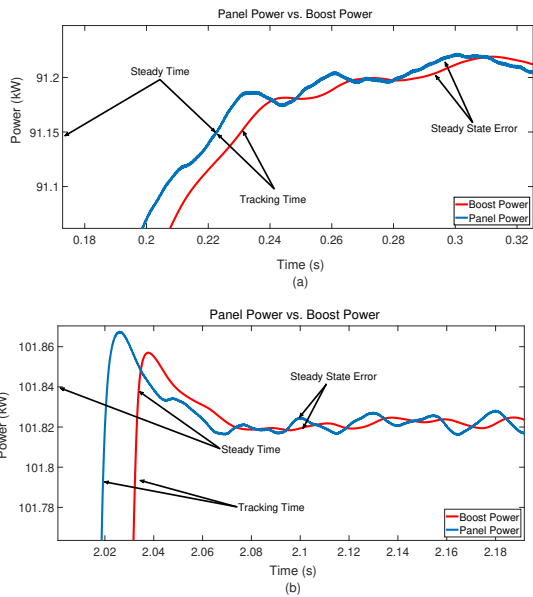


FIGURE 16. Errors between panel power and boost power at 40°C (a) and 20°C (b).

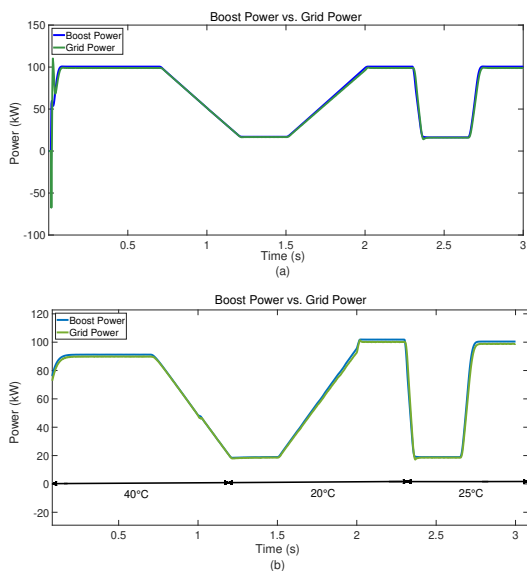


FIGURE 17. Simulation results of boost power and grid power at 25°C (a) and 40°C, 20°C, 25°C (b).

VII. EXPERIMENTAL RESULTS

In this paper, a *HRFLC*-based *MPPT* controller connected to grid with only one input is developed. More specifically, here, the variation of irradiance and temperature in time has been taken into account. Note that three temperatures has been studied 40°C, 25°C, and 20°C. An excellent tracking between the power grid and the *PV* panel power was achieved as reported in Fig. 21, 22, 23 for the 25°C; in Fig. 24 (a) and Fig. 24 (b) for 40°C and 20°C, respectively. In addition, a complete adaptation was observed in the results related to the *PV* panel power and the boost power as illustrated in Figs 13,

14 and 15 for the 25°C; Fig. 16 (a) and 16 (b) for 40°C and 20°C, respectively. It is worth mentioning that a fast reaction and adaptation to different working conditions was observed. In Fig. 24 (a), with the proposed *HRFLC*, the efficiency was 98.83kW power transmission from the *PV* panel to grid out of 100.65 kW, meaning 98.19% of transmitted power for 25°C, 89.8kW for 40°C and 100.2kW for 20°C as illustrated in Fig. 24 (b). The variation of the duty cycle was between only two values: 0.463 and 0.478 to get the highest and lowest irradiance, respectively.

For the power transferred from the panel to the grid in the case of 25°C the tracking time error was about 0.005s as shown in Fig. 23. Fig. 22 depicts a steady state error of 1.82 kW and a steady time of about 0.09s. Since the panel power was 100.65kW, the steady state error was 1.8% (or 98.19% tracking efficiency). Hence, for 20°C and 40°C the tracking times were 0.02s and 0.04s respectively; whereas, the steady state error were 1.8kW and 1.4kW, respectively. It is to be noted that even the steady state error for 40°C was less than 20°C the power transmitted from the panel to the grid was higher than those achieved in 40°C (i.e., 100.2kW and 89.8kW respectively). As regards *PV*-Boost simulations high accuracy and efficiency were reported (Fig. 13 - 15). The tracking time was 0.009s, the steady state error was 0.12 kW and the transit time was 0.08s for 25°C. For 20°C and 40°C the efficiencies are 99.99% and 90.7% respectively. This was due to: i) the use of few *MFs* which reduce the calculation time of the output; ii) the adequate, simple and fast choice of the duty cycle *D* by only two *MFs*. In relation to the results obtained between the boost and the grid at 25°C, a transit time of about 0.01s and a tracking time of 0.004s, were achieved (Fig.19). In Fig.18 the steady state error was of 1.71 kW which means an error of 1.69% for 20°C and 40°C. Fig. 20 (a) and (b) report, instead, the efficiency values that are 99.51% and 89.7% respectively. Most state-of-the-art works performed simulations at 25°C. For example, in [31], the best fuzzy system reported a transit time of 0.91s, a tracking accuracy of 99.93% with an error of 5.86Wh and a steady state error of 0.37%. The *P&O* (0.5%) in [31] reported a transit time of 0.25s and a steady state error of 7.16%. The *ANNs* used in the literature, the steady state error was approximately 3W for 30W (10% of error) [52]. The *ANN*-based system proposed in [53] provided a transit time of 0.05s with a steady state error of 0.6%. In [54] the proposed fuzzy system reported a transit time of 0.25s, and a mean steady state error of 2.36%. In [22] using adaptive neuro-fuzzy controller the steady state error was about 0.5%. In [24] the tracking time error estimated was 1.58s. For further evaluation, Table 3 illustrates the results presented in [45]– [46] such as Third Order B-spline Adaptive Neuro-fuzzy Controller (*TOANC*), fuzzy logic controller, *PID*-incremental conductance (*PID-InCon*) and *PID*-Hill climbing (*PID-HC*). As can be observed, *TOANC* achieved the highest efficiency and the lowest error as it employed the *MPPT* error and its derivative.

Kamal et al. [45]– [46] compared the proposed method

TABLE 3. Summary of the comparative study

Controllers	Efficiency %	Error %
TOANC	99.12	0.88
FLC	91.51	8.49
PID-IC	87.67	12.33
PID-HC	84.01	15.99

TABLE 4. Comparison of power efficiencies

Controllers	Efficiency%	Error %
TOANC	99.12	0.88
Sliding mode controller	97.30	2.7
Integral Backstepping controller	98.04	1.96
Predictive	95.80	4.20
MPPT with irradiance sensor	98.62	1.38
P&O-ANFIS	85-97	15-3
Three-point weighted	96.00	4.00

TOANC with sliding mode controller, integral backstepping controller, predictive, MPPT with irradiance sensor, ANFIS and three point weighted. Comparative results are reported in Table 4. Hence, the proposed HRFLC-based MPPT, which achieved an efficiency of 99.12%, with only one input, one output, and two rules. This FLC can be easily implemented and widely used. Results are summarized Table 5.

The results achieved for 20°C and 40°C are reported in Table 6.

The proposed HRFLC provided high performances with a reduced number of MFs and rules, making its architecture very simple. In fact, the main idea was to keep the voltage stable while the current control the irradiance variation. The choice of the single input ΔI simplifies considerably the implementation. The reasons of using ΔI can be summarized as follows: first, the voltage of the VSC must be kept constant and stable in order to supply the grid with fixed AC voltage.

TABLE 5. Summary of the comparative studies.

Controllers	Inputs	Steady State error	Tracking time	Architecture	Implementation
P&O	ΔP and ΔV	until 10%	0.25s	Very Easy	Very Easy
ANN	GMPP and VGMPP	0.6%	0.05s	Difficult	Difficult
Neuro-Fuzzy	E and ΔE	0.5%	0.5s	Heavy	Difficult
Fuzzy	ΔP and ΔV	0.37%	0.91s	Quite Easy	Quite Easy
TOANC	W and ΔW	0.88%	/	Heavy	Difficult
HRFLC	ΔI	0.119%	0.008s	Very Easy	Very Easy

TABLE 6. Results achieved for simulations carried out at 20°C and 40°C.

	40°C			20°C		
	PP/BP	BP/GP	PP/GP	PP/BP	BP/GP	PP/GP
IE	9.5kW	/	/	≈0	/	/
SSE	0.01kW	1.4kW	1.4kW	0.005kW	2kW	1.8kW
TT	0.01s	0.03s	0.04s	0.01s	0.005s	0.02s
ST	0.22s	0.17s	0.17s	0.04s	0.02s	0.02s

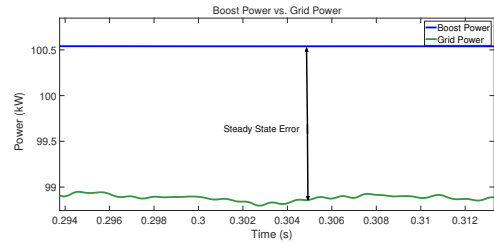


FIGURE 18. Simulation results of the steady state error between the grid power and boost power at 25°C.

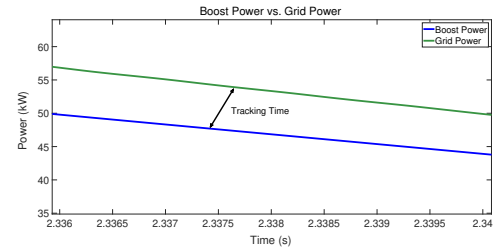


FIGURE 19. Simulation results of the tracking time between the grid power and boost power at 25°C.

Second, the current is more sensible in the B-C zone than the other zones as this work deals with Boost controller. Third, components, time and memory are reduced significantly.

VIII. CONCLUSIONS

In this work, an HRFLC-based MPPT method is proposed as an accurate, simple and representative approach. The design and simulation of the method are discussed in detail. In this paper, only the current variation is used under different weather conditions (i.e., irradiation at 20°C, 25°C and 40°C), achieving high accuracy and efficiency, by employing a number of inputs less than usually used in the literature, mainly twenty-five rules or over. This reduction means that the calculation is simplified significantly. Comparing to the conventional P&O method, the proposed MPPT method can satisfactorily address the trade-off between the tracking speed and steady state oscillations. Moreover, a connection to a grid is achieved. This connection provided high performances. Moreover, the use of Fuzzy in MPPT control (HRFLC) achieves better results than the classical approach, especially for static error and tracking time. Furthermore, in comparison with other controllers like fuzzy, ANNs and so on, the HRFLC reported higher accuracy and efficiency in tracking time, transit time, and steady state with a high reduction in variables and functions. This reduction allows not only to simplify the implementation process but also to achieve a significant gain in terms of time and cost (by using a smaller number of components). This will make an easy process for installation and maintenance. As an alternative perspective, in the future, exploitation of deep and/or reinforcement learning methods [13]– [18], [55] will be also

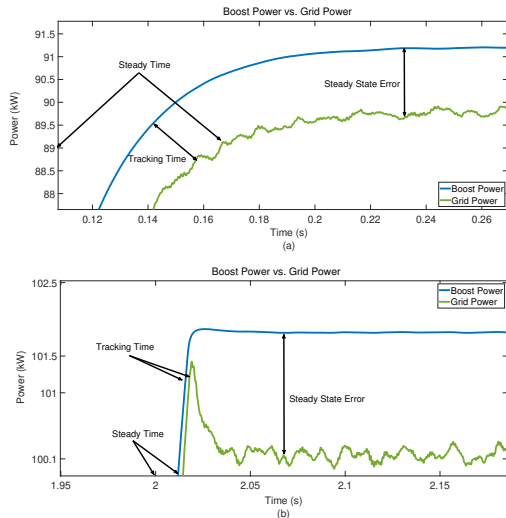


FIGURE 20. Errors between boost power and grid power at 40°C (a) and 20°C (b).

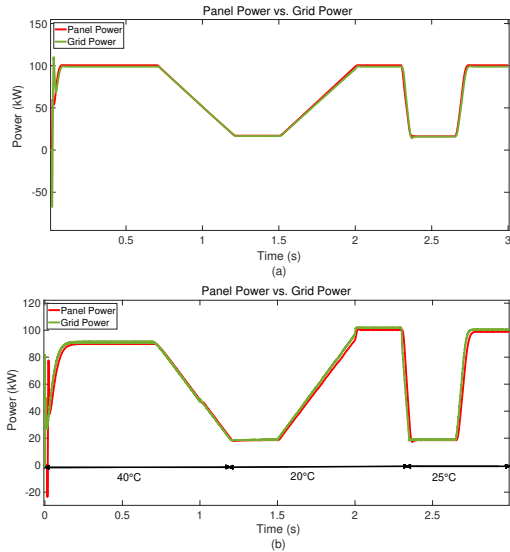


FIGURE 21. Simulation results of panel power and grid power at 25°C (a) and 40°C, 20°C, 25°C (b).

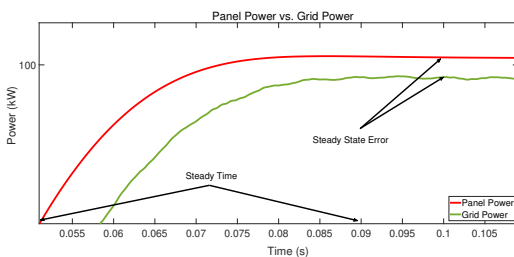


FIGURE 22. Simulation results of the steady time and steady state error of the grid power and PV Panel power at 25°C.

explored.

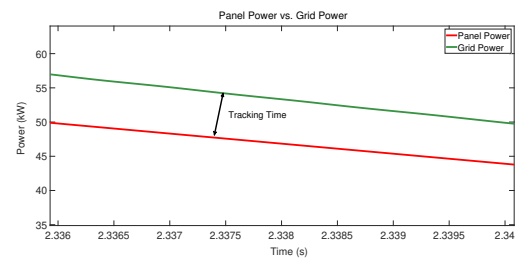


FIGURE 23. Simulation results of the tracking time between the grid power and PV panel power at 25°C.

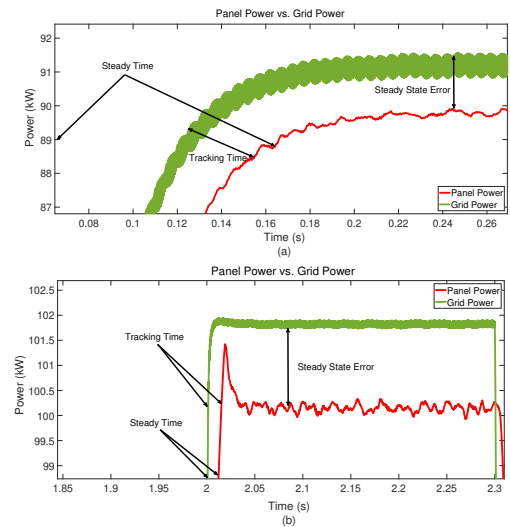


FIGURE 24. Errors between panel power and grid power at 40°C (a) and 20°C (b).

REFERENCES

- [1] J. Ahmed and Z. Salam, "A Modified P&O Maximum Power Point Tracking Method with Reduced Steady State Oscillation and Improved Tracking Efficiency," *IEEE Transactions on Sustainable Energy*, vol. 7, no. 4, pp. 1506-1515, 2016.
- [2] H.T. Yau, C.H. Wu, "Comparison of extremum-seeking control techniques for maximum power point tracking in photovoltaic systems," *Energies*, vol. 4, pp. 2180-2195, 2011.
- [3] C. Li, Y. Chen, D. Zhou, J. Liu, J. Zeng, "A High-Performance Adaptive Incremental Conductance MPPT Algorithm for Photovoltaic Systems," *Energies*, vol. 9, no. 4, pp. 288, 2016.
- [4] Y. Sun, S. Li, B. Lin, X. Fu, M. Ramezani, and I. Jaithwa, "Artificial Neural Network for Control and Grid Integration of Residential Solar Photovoltaic Systems," *IEEE Transactions on Sustainable Energy*, vol. 8, no. 4, pp. 1484-1495, 2017.
- [5] M.A. Elgendy, B. Zahawi, D.J. Atkinson, "Assessment of Perturb and Observe MPPT Algorithm Implementation Techniques for PV Pumping Applications," *IEEE Transactions on Sustainable Energy*, vol.3, no. 1, pp.21-33, 2012.
- [6] S. Strache, J.H. Mueller, D. Platz, R. Wunderlich, S. Heinen, "Maximum power point tracker for small number of solar cells connected in series," *IECON 2012 - 38th Annual Conference on IEEE Industrial Electronics Society*, vol., no., pp.5732,5737, 25-28 Oct. 2012.
- [7] J.T. Bialasiewicz, "Renewable Energy Systems With Photovoltaic Power Generators: Operation and Modelling. Industrial Electronics," *IEEE Transactions on Industrial Electronics*, vol.55, no.7, pp. 2752-2758, 2008.
- [8] Y. Jiang, J.A.A. Qahouq, T.A. Haskew, "Adaptive step size with adaptive-perturbation-frequency digital MPPT controller for a single-sensor photovoltaic solar system," *IEEE Trans. Power Electron.*, vol. 28, pp. 3195-3205, 2013.

- [9] S.K. Kollimalla and M.K. Mishra, "Variable perturbation size adaptive P&O MPPT algorithm for sudden changes in irradiance," *Sustainable Energy, IEEE Transactions on*, vol. 5, pp. 718-728, 2014.
- [10] Q. Mei, M. Shan, L. Liu, J.M. Guerrero, "A novel improved variable step-size incremental-resistance MPPT method for PV systems," *IEEE Trans. Ind. Electron.*, vol. 58, pp. 2427-2434, 2011.
- [11] A.I. Dounis, P. Kofinas, C. Alafodimos, D. Tseles, "Adaptive fuzzy gain scheduling PID controller for maximum power point tracking of photovoltaic system," *Renew. Energy*, vol. 60, pp. 202-214, 2013.
- [12] M. Mazandarani and L. Xiu, "Fractional Fuzzy Inference System: The New Generation of Fuzzy Inference Systems," *IEEE Access*, vol. 8, pp. 126066 - 126082, 2020.
- [13] M. Mahmud, M.S. Kaiser, A. Hussain and S. Vassanelli, "Applications of Deep Learning and Reinforcement Learning to Biological Data. in *IEEE Transactions on Neural Networks and Learning Systems*," vol. 29, no. 6, pp.2063-2079, 2018.
- [14] C. Ieracitano, N. Mammone, A. Hussain, and F. C. Morabito, "A novel multi-modal machine learning based approach for automatic classification of EEG recordings in dementia," *Neural Networks*, vol. 123, pp. 176-190, 2020.
- [15] N. Mammone, C. Ieracitano, and F.C. Morabito, "A deep CNN approach to decode motor preparation of upper limbs from time-frequency maps of EEG signals at source level," *Neural Networks*, vol. 124, pp.357-372, 2020.
- [16] Z.K. Malik, A. Hussain and J. Wu, "Multi-Layered Echo State Machine: A novel Architecture and Algorithm for Big Data applications," *IEEE Transactions on Cybernetics*, vol. 47, no. 4, pp. 946 - 959, 2017.
- [17] F. Xiong, B. Sun, X. Yang, H. Qiao, K. Huang, A. Hussain, Z. Liu, "Guided Policy Search for Sequential Multitask Learning," in *IEEE Transactions on Systems, Man, and Cybernetics: Systems*, vol. 49, no. 1, pp. 216-226, 2019.
- [18] X. Yang, K. Huang, R. Zhang, A. Hussain, "Learning Latent Features with Infinite Non-negative Binary Matrix Tri-factorization," *IEEE Transactions on Emerging Topics in Computational Intelligence*, vol. 2, no. 5, pp. 450-463, 2018.
- [19] M.S. Kaiser, Z. Chowdhury, S. Mamun, A. Hussain and M. Mahmud, "A Neuro-Fuzzy Control System Based on Feature Extraction of Surface Electromyogram Signal for Solar-Powered Wheelchair," *Cogn. Comput.*, vol. 8, no. 5, pp. 946-954, 2016.
- [20] M. Mahmud et al., "A Brain-Inspired Trust Management Model to Assure Security in a Cloud Based IoT Framework for Neuroscience Applications," *Cogn. Comput.*, vol. 10, no. 5, pp. 864-873, 2018.
- [21] H. Seiti and A. Hafezalkotob, "A New Risk-Based Fuzzy Cognitive Model and Its Application to Decision-Making," *Cogn. Comput.*, vol. 12, pp. 309-326, 2020.
- [22] M. Mahdavi, L. Li, J. Zhu, and S. Mekhilef, "An Adaptive Neuro-Fuzzy Controller for Maximum Power Point Tracking of Photovoltaic Systems," *TENCON 2015 - 2015 IEEE Region 10 Conference* https://umexpert.um.edu.my/file/publication/00005361_133573.pdf
- [23] S. S. Mohammed, D. Devaraj, T.P.I. Ahamed, "Maximum Power Point Tracking System for Stand Alone Solar PV Power System Using Adaptive Neuro-Fuzzy Inference System," 2016 Biennial International Conference on Power and Energy Systems: Towards Sustainable Energy (PESTSE) 978-1-4673-6658-8/16/\$31.00 2016 IEEE
- [24] A. Bin-Halabi, A. Abdennour, H. Mashaly, "An Accurate ANFIS-based MPPT for Solar PV System," *International Journal of Advanced Computer Research*, vol. 4, no. 2, pp.588, 2014.
- [25] S. Tang, Y. Sun, Y. Chen, Y. Zhao, Y. Yang, and Warren Szeto, "An Enhanced MPPT Method Combining Fractional-Order and Fuzzy Logic Control," *IEEE J. Photovoltaics*, vol. 7, no. 2, pp. 640-650, 2017.
- [26] L.K. Letting, J.L. Munda, Y. Hamama, "Optimization of a fuzzy logic controller for PV grid inverter control using S-function based PSO," *Sol. Energy*, vol. 86, pp. 1689-1700, 2012.
- [27] M.M. Algazar, H. AL-monier, H.A. EL-halim, M.E.E.K. Salem, "Maximum power point tracking using fuzzy logic control," *Int. J. Electr. Power Energy Syst.*, vol. 39, pp. 21-28, 2012.
- [28] B.N. Alajmi, K.H. Ahmed, S.J. Finney, B.W. Williams, "Fuzzy-logic-control approach of a modified hill-climbing method for maximum power point in microgrid stand alone photovoltaic system," *IEEE Trans. Power Electron.*, vol. 26, pp. 1022-1030, 2011.
- [29] B.N. Alajmi, K.H. Ahmed, S.J. Finney, B.W. Williams, "A maximum power point tracking technique for partially shaded photovoltaic systems in microgrids," *IEEE Trans. Ind. Electron.* vol. 60, pp. 573-584, 2011.
- [30] C.B. Salah, M. Ouali, "Comparison of fuzzy logic and neural network in maximum power point tracker for PV systems," *Electr. Power Syst. Res.*, vol. 81, no. 1, pages 43-50, 2011.
- [31] L. Chun-Liang, C. Jing-Hsiao, L. Yi-Hua, and Y. Zong-Zhen, "An Asymmetrical Fuzzy-Logic-Control-Based MPPT Algorithm for Photovoltaic Systems," *Energies*, vol. 7, pp. 2177-2193, 2014.
- [32] S. Jaw-Kuen, W. Yu-Chen, and C. Bo-Chih, "A Study on the Fuzzy-Logic-Based Solar Power MPPT Algorithms Using Different Fuzzy Input Variables," *Algorithms*, vol. 8, pp. 100-127, 2015.
- [33] T. Krishna Mohan, Sk. Faiz Mohammed, "A Neuro-Fuzzy Controller for Multilevel Renewable Energy System," *International Conference on Electrical, Electronics, and Optimization Techniques (ICEEOT)*, pp. 4120-4123, 2016.
- [34] M. Barsacchi, A. Bechini, P. Ducange, and F. Marcelloni. "Optimizing Partition Granularity, Membership Function Parameters, and Rule Bases of Fuzzy Classifiers for Big Data by a Multi-objective Evolutionary Approach," *Cogn Comput*, vol. 11, no. 3, pp. 367-387, 2019.
- [35] S. López, A. A. Márquez, F. A. Márquez, and A. Peregrín, "Evolutionary Design of Linguistic Fuzzy Regression Systems with Adaptive Defuzzification in Big Data Environments," *Cogn Comput*, vol. 11, no. 3, pp. 388-399, 2019.
- [36] L. Zhang and Y. He, "Extensions of Intuitionistic Fuzzy Geometric Interaction Operators and Their Application to Cognitive Microcredit Origination," *Cogn Comput*, vol. 11, no. 5, pp. 748-760, 2019.
- [37] X. Tang and G. Wei, "Multiple Attribute Decision-Making with Dual Hesitant Pythagorean Fuzzy Information," *Cogn Comput*, vol. 11, no. 2, pp. 193-211, 2019.
- [38] G. Sun, X. Guan, X. Yi, and Z. Zhou, "Improvements on Correlation Coefficients of Hesitant Fuzzy Sets and Their Applications," *Cogn Comput*, vol. 11, no. 4, pp. 529-544, 2019.
- [39] L.M. Elobaid, A.K. Abdelsalam, and E.E. Zakzouk, "Artificial Neural Network Based Maximum Power Point Tracking Technique for PV Systems," *IECON 2012 - 38th Annual Conference on IEEE Industrial Electronics Society* Pp:937-942, 2012.
- [40] A.M. Ameen, J. Pasupuleti, T. Khatib, W. Elmenreich, H.A. Kazem, "Modeling and Characterization of a Photovoltaic Array Based on Actual Performance Using Cascade-Forward Back Propagation Artificial Neural Network," *J. Sol. Energy Eng.*, vol. 137, no. 4, pp. 041010.
- [41] E. Karatepe, T. Hiyama, "Artificial neural network-polar coordinated fuzzy controller based maximum power point tracking control under partially shaded conditions," *IET Renew. Power Gener.*, vol. 3, no. 2, pp. 239-253, 2009.
- [42] V. Salas, E. Olias, Alasaro, A. Barrado, "New algorithm using only one variable measurement applied to a maximum point tracker," *Solar Energy Materials and Solar Cells*, vol. 87, no. 1-4, pp. 675-684, 2005.
- [43] S. Berlin Jeyaprabha and A. Immanuel Selvakumar, "Model-Based MPPT for Shaded and Mismatched Modules of Photovoltaic Farm," *IEEE Transactions on Sustainable Energy*, vol. 8, no. 4, pp. 1763-1771, 2017.
- [44] N.S. D'Souza, L.A.C. Lopes, X. Liu, "Comparative study of variable size perturbation and observation maximum power point trackers for PV systems," *Electr. Power Syst. Res.*, vol. 80, pp. 296-305, 2010.
- [45] T. Kamal, M. Karabacak, F. Blaabjerg, S.Z. Hassan, L.M. Fernández-Ramírez, "A novel Lyapunov stable higher order B-spline online adaptive control paradigm of photovoltaic systems," *Solar Energy*, vol. 194, pp. 530-540, 2019.
- [46] T. Kamal, M. Karabacak, S.Z. Hassan, H. Li and L.M. Fernández-Ramírez, "A Robust Online Adaptive B-spline MPPT Control of Three-Phase Grid-Coupled Photovoltaic Systems under Real Partial Shading Condition," *IEEE Transactions on Energy Conversion*, vol. 34, no. 1, pp. 202-210, 2018.
- [47] A. Haque, "Maximum Power Point Tracking (MPPT) Scheme for Solar Photovoltaic System," *Energy Technology & Policy*, vol. 1, no. 1, pp. 115-122, 2014.
- [48] M. Merenda, D. Iero, R. Carotenuto, and F.G. Della Corte, "Simple and Low-Cost Photovoltaic Module Emulator," *Electronics*, vol. 8, no. 12, pp. 1445, 2019.
- [49] S.K. Chattopadhyay and C. Chakraborty, "A New Asymmetric Multilevel Inverter Topology Suitable for Solar PV Applications with Varying Irradiance," *IEEE Transactions on Sustainable Energy*, vol. 8, no. 4, pp. 1496-1506, 2017.
- [50] K.R.M.N. Ratnayake, Y. Murai and T. Watanabe, "Novel PWM Scheme to Control Neutral Point voltage Variation in Three-Level Voltage Source Inverter," *IEEE, Industry Applications Conference*, vol. 3, pp. 1950-1955, 1999.

- [51] A. Rufer, "An aid in the teaching of multilevel inverters for high power applications," Proceedings of the Power Electronics Specialists Conference, pp. 347-352, 1995
- [52] H. Zhang and S. Cheng, "A New MPPT Algorithm Based on ANN in Solar PV Systems," Advances in Computer, Communication, Control & Automation, LNEE 121, pp. 77-84, 2011.
- [53] L. Bouselham, M. Hajji, B. Hajji and H. Bouali, "A MPPT-Based ANN Controller Applied To PV Pumping System," Renewable and Sustainable Energy Conference (IRSEC), 2016.
- [54] A.A.S. Mohamed, A. Berzoy and O. Mohammed, "Design and Hardware Implementation of FL- MPPT Control of PV Systems Based on GA and Small-Signal Analysis," IEEE Transactions on Sustainable Energy, vol. 8, no. 1, pp. 279-290, 2016.
- [55] C. Ieracitano, N. Mammone, A. Bramanti, A. Hussain, and F.C. Morabito, "A Convolutional Neural Network approach for classification of dementia stages based on 2D-spectral representation of EEG recordings," Neurocomputing, vol. 323, pp. 96-107, 2019.



ABDEFATEH KERROUCHE received his PhD degree "Measurement and Instrumentation" from City University London in 2009, funded by funded by Sustainable Bridges EU Project. He was awarded the degrees of Master of philosophy in Electronics from Pierre & Marie Curie Paris VI University (France) and a Master of Electronics from Marne-La-Vallee University, France. From 2010 to 2015, he worked as a research associate at Heriot Watt University (2010-2015). He developed 3D ray-tracing models for Luminescent Solar Concentrators and he designed systems for water sampling and pathogen detection within Aqua Valens EU Project. Since 2016, He is a Lecturer and Sensors/Systems Consultant at Edinburgh Napier University. He has published more than 15 papers in reputed journals and international conferences. His area of interest includes: Pathogen detection, Water sample preparation, Sensors, Aquaculture and Renewable Energy.



FARAH LOTFI received the B.Eng. and D. degrees in Arabic handwritten recognition from the University of Badji Mokhtar Annaba, Algeria, in 1995 and 2000, respectively. From 2000 to 2012, he was a Research Associate with the University of Cherif Messadia, Algeria. He is currently a Research with Badji Mokhtar University in Génie Electromécanique Laboratory, Annaba, Algeria. His current research interests include AI, Fuzzy System, Neural Network and Photovoltaic model-

ing and control, energy conversion and power electronics. He has authored and co-authored different seminar papers. Dr. Lotfi has reviewed for international journals in his research field, AI, such as Journal of Environmental Progress & Sustainable Energy Wiley and Computer Science USA.



COSIMO IERACITANO received the Master's degree (summa cum laude) in electronic engineering and Ph.D. degree (with the additional label of Doctor Europaeus) from the University Mediterraena of Reggio Calabria (UNIRC), Italy, in 2013 and 2019, respectively. He was a Visiting Master Student at ETH Zurich and a Visiting PhD Student at the University of Stirling in 2013 and 2018, respectively. He is author/co-author of publications in peer-reviewed national/international journals and conference contributions. His main research interests include:

information theory, machine learning, deep learning techniques and biomedical signal processing, in particular EEG signals of subjects affected by neuropathologies.



AMIR HUSSAIN (SM'97) received the BEng (Highest First Class Hons.) and PhD degrees in novel neural network architectures and algorithms from the University of Strathclyde, Glasgow, UK, in 1992 and 1997, respectively. He was a Research Fellow with the University of Paisley (currently, the West of Scotland), Paisley, UK, from 1996 to 1998, and a Research Lecturer with the University of Dundee, Dundee, UK, from 1998 to 2000. He joined the University of Stirling, Stirling, UK,

in 2000, where he is currently a Professor of Cognitive Computing, and the Founding Director of the Cognitive Big Data Informatics Laboratory. His current research interests include next generation brain-inspired multimodal cognitive technology for solving complex real-world problems, such as medical and social multimedia big data analytics, visualization, sentiment and opinion mining, personalized and preventative (e-and m-) health- care, cognitive agent-based complex autonomous systems, cognitive hearing systems, and assistive technology and related clinical research. He has published nearly 300 papers, including over a dozen books and 80 journal papers in the above areas. Prof. Hussain is the Founding Editor-in-Chief of Cognitive Computation (Springer-Nature) and Big Data Analytics (BioMed Central), and the Chief-Editor of the Springer Book Series on Socio-Affective Computing, and Springer Briefs on Cognitive Computation. He is an Associate Editor of the IEEE Transactions on Neural Networks and Learning Systems, a member of several Technical Committees of the IEEE Computational Intelligence Society, the Founding Publications Co-Chair of the International Neural Network Society Big Data Section, and the Chapter Chair of the IEEE U.K. and RI Industry Applications Society.



JAMIL AHMAD received his PhD in Artificial Neural Network from Department of Electrical and Electronics Engineering, Kings' College London, UK, MSc in Information Technology from University of Warwick, UK, and MSc in Computer Science from University of Peshawar. He has over 22 years of Post-PhD experience of Administration, Research, Teaching, and project management at various international academic institutions. He published over 110 papers/book chapters in the

areas of Science, Engineering and Technology in international journals and refereed conferences. Obtained grants for research and academic projects from various organizations including National Information and Communication Technology (ICT) R&D Fund Pakistan, HEC-British Council linkage program, and the UK Government under PMI 2 program. He was also honored with the award of Charles Wallace Pakistan Trust Visiting fellowship, UK (2012-13) and International Visiting Leadership Program (IVLP) fellowship (August – September 2007), USA. He is a Fellow of the British Computer Society, Senior Member of IEEE, CEng, Member IET and Member ACM. Currently, he is holding the position of Vice Chancellor Kohat University of Science and Technology (KUST) Kohat, Khyber Pakhtunkhwa (KPK). Pakistan.



MUFTI MAHMUD (GS'08-M'11-SM'16) received the Ph.D. degree in information engineering from the University of Padova, Padua, Italy, in 2011. He is currently a Senior Lecturer with the Department of Computing and Technology, School of Science and Technology, Nottingham Trent University, U.K. With over 70 peer-reviewed research articles, his current research interests include neuroscience big data analytics, the Internet of healthcare things, and trust management in cyber-physical systems. He was a recipient of the Marie-Curie Fellowship. He also serves at various capacities in the organization of leading conferences, including the Coordinating Chair of the local organization committee of the IEEE WCCI2020 conference and a General Chair of the Brain Informatics 2020 conference. He serves as Editorial Board Member of Cognitive Computation (Springer-Nature) and Big Data Analytics (BioMed Central, Springer-Nature) journals, and an Associate Editor of Brain Informatics (SpringerOpen) and IEEE ACCESS journals.

• • •